



Fatigue Crack Growth Estimation in Low-Alloy Steel Under Random Loading in Middle Section of Fatigue Diagram

A. N. Savkin, A. A. Sedov, and K. A. Badikov(✉)

Volgograd State Technical University (VSTU), 28, Lenina St, Volgograd 400005, Russian Federation

Abstract. The fatigue crack growth kinetics were studied under regular and irregular cyclic loading with different asymmetry ratios, as well as spectral loading typical for the operation of various structural objects, in the middle section of the fatigue crack growth diagram on $C(T)$ type specimens cut from low-alloy steel used in the automotive industry. The R -ratio of different levels influence and irregular loading character on the fatigue crack growth duration at different values of maximum loading is shown. A model of the crack growth duration is proposed on the basis of considering the “crack closure,” and for irregular cyclic loading, in addition, the character of variable amplitude loading with its reduction to an equivalent regular loading. This made it possible to reduce the fatigue crack growth diagrams group with different asymmetry ratios to one equivalent curve. The forecasting of the fatigue crack growth duration was carried out by the cyclic calculation method (“cycle-by-cycle”) and by the proposed empirical dependence.

Keywords: Regular and irregular cyclic loading · Low-alloy steel · Crack growth life model

1 Introduction

While in operation, vehicles experience variable loads from various types of road surfaces, maneuvering during movement, changes in temperature conditions, impact action in the obstacle crossing process. It leads to fatigue damage accumulation in the load-bearing design elements, leading to the fatigue cracks growth. Microcracks are formed in stress raiser of a part, and it is often difficult to detect them without special equipment. Gradually, this process takes on the character of an avalanche effect, and the part may be destroyed.

To prevent such a scenario, it is necessary, knowing where such fatigue cracks can occur, to check the maintenance inspection to detect them. To establish the examination of such rates, it is necessary to know the crack growth kinetics so that the emerging crack can be detect before its critical growth.

In the suggested work, on the low-alloy steel specimens used in the automotive components production, and the fatigue crack kinetics growth analysis under regular

and irregular loading is carried out, considering the effect on of different asymmetry ratio R and maximum loading P_{max} . Irregular loading is modeled based on standard random spectra using in the engineering design of automotive load-bearing structural elements.

2 Material, Research Technique

The compact specimens $60 \times 62.5 \times 5$ mm in size with an edge crack are investigated, cut from low-alloy steel, close to the analog Russian steel—09G2. This alloy is used in the automotive industry, concretely for the manufacture of front suspension for passenger cars [1–5].

The thickness of this material specimen is 5 mm that give it possible to assert that the fatigue crack propagation under a plane stress condition. The drawing is shown in Fig. 1.

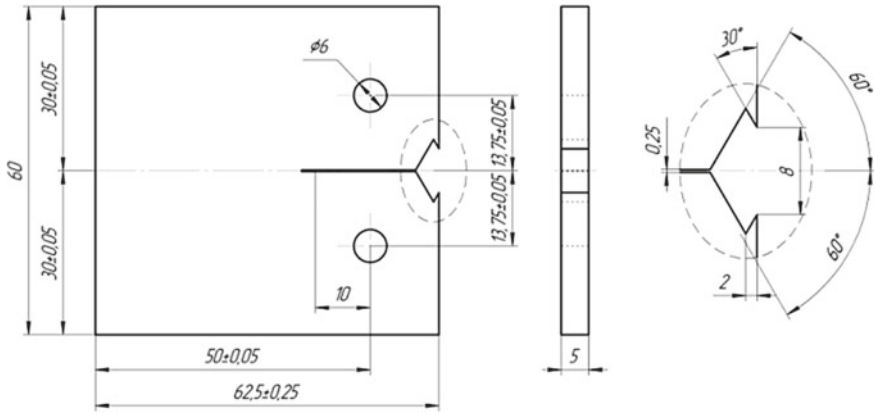


Fig. 1 Geometry of test specimen

Chemical composition of the alloy % (mass): Fe 98.7; C 0.078; Cr 0.1; Cu 0.016; Mn 0.96; Nb 0.04; Si 0.1; Ti 0.016; Al 0.036. Mechanical properties of alloy: ultimate strength $\sigma_u = 496$ MPa, conditional yield strength $\sigma_y = 345$ MPa, modulus of elongation $E = 210$ GPa.

Experimental studies were carried out using specialized software MTL-32, controls the test under load control mode. VAFCP (Variable Amplitude Fatigue Crack Propagation) software, which allows testing under various loading conditions in automatic mode, including loading level control to provide a set value of K , as well as automatic recording of the crack length and other test results. The compliance method was used to measure crack length, using the BISS Bi-06–201 Crack Opening Displacement (COD) gauge, which measures distance between edges of the specimen. The tests were carried out in air under normal ambient conditions, and the frequency of the main type of loading was 10 Hz. The test procedure conforms to the specification of ASTM E 647–08. The crack growth kinetics were recorded depending on the number of cycles during the test.

The crack resistance testing program consists of testing at constant amplitude (CAL) and variable amplitude loading (VAL) with different asymmetry ratio R from 0 to 0.75 and a maximum load of 3.5–7 kN. For variable amplitude tests, spectra of a quasi-random nature are formed on the basis of standard loading spectra typical for variable loading of various technical objects and contractual elements [6–10]. Figure 2 shows examples of normalized loading spectra.

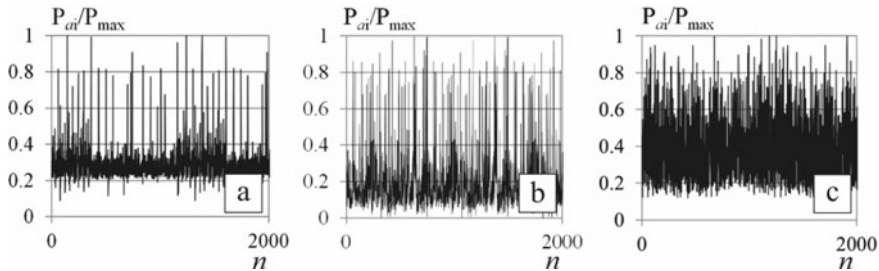


Fig. 2 Examples of selection from normalized loading spectra: **a**—SAESUS; **b**—SAE-TRANS; **c**—SAEBRACKET

SAESUS, SAEBRACKET, SAETRANS spectra—shortened load front suspension spectrums, brake gear and transmission of a passenger car. Model spectra A and C are formed on the basis of an autocorrelation approach for the Rayleigh distribution, which is most typical for failures of technical objects and constructions fatigue-prone and wear [11–13]. The test schedule is shown in Table 1. Before testing, the fatigue crack was performed by precracking to a value of $a_0 = 15$ mm under constant amplitude loading with a nominal load at $R = 0$, $P = 0.6 \cdot P_{\max}$ from the subsequent test. The critical size, of the crack length corresponding to the specimen failure at the provided tests, is $a_{\text{cr}} = 31\text{--}34$ mm.

3 Research Results

Figure 3 shows the test results (Fig. 3a). Based on the dependences of the crack growth kinetics $a\text{-lg}N$, obtained using a crack opening displacement gauge, the testing machine software automatically estimates the growth rate da/dN and the amplitude of the stress intensity factor (SIF) ΔK at the crack mouth. These results make it possible to plot the fatigue diagrams. Item numbers in Fig. 3 correspond to those numbers in Table 1.

Test results at different types of loading and different values of the asymmetry ratio of the loading block $R = 0\text{--}0.75$ show that all fatigue diagram curves have tendency to parallelism in logarithmical coordinates ($\lg(da/dN)\text{-}\lg(\Delta K)$). Comparison of tests under constant amplitude loading is carried out with the same P_{\max} but different R , and show that an asymmetry ratio increasing leads to an increase in crack growth life, because of a decrease in the range of the ΔK . In Fig. 3a, it can be seen that at a constant $P_{\max} = 5$ kN and $R \leq 0.5$ for a given material, the rate hardly exceeds 300 thousand cycles, and at $R \geq 0.7$ the durability essentially increases to million cycles.

Table 1 Test schedule

Loading	P_{max} , kN	R	V	K	N_{EXP} million cycles	N_{VAL} , million cycles	N_{CYC} , million cycles	Position in Fig. 3
CAL	5	0	1	1	0.080	-	0.063	1
	5	0.1	1	1	0.062	-	0.073	2
	5	0.3	1	1	0.118	-	0.112	3
	5	0.5	1	1	0.310	-	0.235	4
	5	0.7	1	1	1.090	-	0.911	5
	5	0.75	1	1	1.701	-	1.553	6
SAETRANS	3.5	0.1	0.381	20	5.300	4.815	7.258	7
	5	0	0.381	20	1.770	1.821	1.733	8
	7	0.1	0.381	20	0.553	0.616	0.627	9
SAEBRACKET	3.5	0.1	0.401	18	3.404	4.319	6.068	10
	5	0	0.401	18	1.277	1.633	1.450	11
	7	0.1	0.401	18	0.488	0.522	0.525	12
SAESUS	3.5	0.1	0.277	32	14.317	8.474	6.289	13
	5	0	0.277	32	5.325	3.204	5.281	14
	7	0.1	0.277	32	1.957	1.083	1.907	15
Spectrum A	7	0.1	0.391	19	0.641	0.583	0.573	16
Spectrum C	7	0.1	0.296	30	1.523	0.977	1.512	17

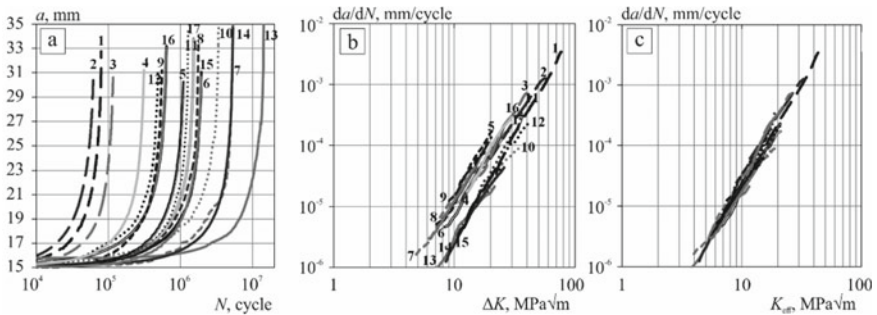


Fig.3 Curves of crack growth (a), experimental (b) and effective SIF (c)

The asymmetry ratio is also influencing on the fatigue diagram position. In Fig. 3b, it is clearly seen that at increase asymmetry ratio, the curves from 1 to 6 are located lower and more to the left. At a constant value P_{max} and regular loading, the range of coefficient ΔK decreases and the duration of crack growth increases. Growth curves and KDFC 5 and 6 in Fig. 3 correspond to tests at asymmetry of 0.7 and 0.75. It is

assumed that at such asymmetries R , the crack closure effect is not observed [14–16], which effects on the crack growth kinetics.

The difference between variable and constant amplitude loading is estimated with measuring of irregularity (completeness). The loading completeness ratio V for the presented tests is shown in Table 1, for constant amplitude loading the completeness ratio is equal to one.

$$V = \left[\frac{1}{v_b} \left[\sum_{i=1}^{v_b} v_{ai} \left(\frac{\Delta P_{ai}}{P_{\max}} \right)^n \right] \right]^{\frac{1}{n}} \tag{1}$$

where v_b, v_a —number of cycles of the sample and block of variable loading with load ΔP_{ai} ; $\Delta P_{ai}/P_{\max}$ —is the normalized i loading amplitude. This approach corresponds to the replacement of variable amplitude loading with equivalent constant ones, corresponding to irregular random loading in terms of the damaged ability. The calculated V ratio is shown in Table 1. It is clearly seen from the position of the initial part of fatigue diagram for different spectra, where, at a decrease V ratio in the SAESUS spectrum, fatigue diagram settle regardless of R and P_{\max} that crack growth life reduces, but retains parallelism in these coordinates, as and fatigue diagrams at CAL. On the fatigue diagram, position of VAL is influenced by the value of the maximum load P_{\max} . At the increase the load from 3.5 to 7 kN and maintaining a low asymmetry $R = 0-0.1$, the fatigue diagram curves shift toward the region of increased crack growth rates. This is clearly seen in the SAESUS spectrum (13–15 curves) and the SAETRANS spectrum (7–9 curves).

Analytical fatigue diagram curves in the middle zone are described by the Paris equation [5]:

$$\frac{da}{dN} = C \cdot \Delta K^n \tag{2}$$

where da/dN is the crack growth rate during the loading cycle; ΔK is the range of SIF; C and n are empirically determined coefficients that are the cyclic crack resistance characteristics of the material. In the present work, for the steel under study, the values $C = 5 \cdot 10^{-14}$ and $n = 3.5$ are obtained to estimate the speed da/dN (mm / cycle) and ΔK in $\text{MPa}\sqrt{\text{mm}}$.

Because the position of the fatigue diagram curves at CAL block (Fig. 3b) significantly depends on the asymmetry ratio R , and the position of the curves at VAL, accept asymmetry, is influenced by the irregularity ratio V ; therefore, in this article, the approach of the effective SIF ΔK_{eff} is used, which makes it possible to approximate these curves to a single curve specific at $R = 0$, which is shown in Fig. 3c.

To consider the phenomenon of “crack closure” [17–21], which occurs when the cycle asymmetry ratio R is less than 0.6–0.7, and which reduces the crack growth rate by reducing the range ΔK , the parameter U is introduced to describe crack closure with an asymmetry of $0.1 \leq R \leq 0.7$ for steels according to the equation in the form of a polynomial dependence:

$$U = 0.57 + 0.16 \cdot R + 0.53 \cdot R^2 - 0.43 \cdot R^3 - 2.58 \cdot R^4 + 6.15 \cdot R^5 - 3.13 \cdot R^6 \tag{3}$$

Thus, in our calculation, the effective SIF at the crack mouth for different types of loading is taken as:

$$\Delta K_{eff} = \Delta K \cdot U \cdot V \tag{4}$$

In this expression, the effect of “crack closure” and the loading cycle asymmetry on the crack growth rate is estimated through the asymmetry ratio R .

4 Results and Discussion

The crack propagation process largely depends on the sequence of loads, which is random. So, the prediction of crack growth is carried out by integration, by the cycle-by-cycle method in the order of the cycles in a random process, starting from the minimum crack length, at which its detection is possible, according to the formula:

$$N_{CYC} = \int_{a_0}^{a_{cr}} \frac{1}{C \cdot \Delta K_{eff}^n} \tag{5}$$

where N_{CYC} —estimated of crack growth life under CAL and VAL by the cycle-by-cycle method; ΔK_{eff} —the effective SIF, determined by Eq. (4); a_0, a_{cr} —initial and critical crack length.

Another approach for estimating of crack growth life at VAL N_{VAL} is based on the proposal to consider the crack growth kinetics on the basis of its growth at CAL N_{CAL} and taking into account the nature of variable loading through the irregularity coefficient V at the same force parameters P_{max} and R without taking into account the interaction of amplitudes in the loading spectrum (6):

$$\begin{aligned} N_{VAL} &= N_{CAL} \cdot K \\ K &= 10^{(1+A \lg n) \cdot (1-V)} \end{aligned} \tag{6}$$

where A —scaling parameter equal to 2 for the studied steel, K —the coefficient of increasing the fatigue crack growth life at VAL compared to CAL with the same loading parameters P_{max} and R .

The calculation results using the methods describe above are shown in Fig. 4 in the form of the calculated values dependence N_{CYC} or N_{VAL} from the experimental N_{EXP} . Comparison of the durability gives good enough agreement between the calculated and experimental data [9, 10].

5 Conclusions

Thus, it has been established that the growth rate and the position of curves on fatigue diagram under VAL are influenced not only by the asymmetry ratio R , as in the case of CAL, but also by the irregularity ratio V , which takes into account the irregularity of random loading.

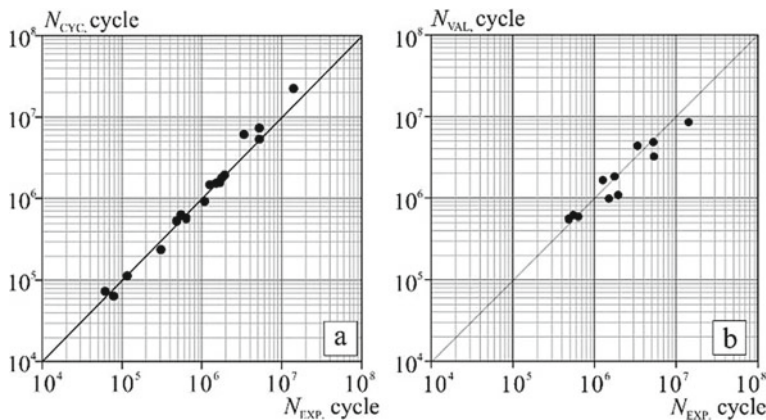


Fig. 4 Calculation of the crack growth life by the cycle method **a** and by formula (6) **b** in comparison with the experiment

The cycle-by-cycle method for predicting the fatigue crack life in steels, considering the effective SIF, show a high convergence of the calculated and experimental values, as well as the approach based on the use of an equivalent constant amplitude loading to predict irregular loading. The correlation coefficient for the first and second methods is $r_2 = 0.99$ and $r_2 = 0.91$, respectively.

References

1. Gouth HJ (1926) The fatigue of metals. Scott, Greenwood, London
2. Furuya Y (2019) Gigacycle fatigue in high strength steels. *Sci Technol Adv Mater* 20(1):643–656
3. Schijve J (2009) Fatigue of structures and materials. Springer, Delft, pp 623
4. Barsom JM (1976) Fatigue crack growth under variable amplitude loading in various bridge steels. In: Fatigue crack growth under spectrum loads, pp 217–232. <https://doi.org/10.1520/STP33374S>
5. Paris PC (1964) The fracture mechanics approach to fatigue, fatigue an interdisciplinary approach. Syracuse University Press, Syracuse, N.Y., pp 107–132
6. Savkin AN, Sedov AA, Denisevich DS, Badikov KA (2018) Crack-tip stress distributions under variable amplitude loading. AIP conference proceedings, pp 2051
7. Johnson HU, Paris PC (1968) The growth of fatigue cracks due to variations in load. *Jorn Fract Mech* 1:1–45
8. Sunder R (2012) Unraveling the science of variable amplitude fatigue. *J ASTM Int* 9(1):32
9. Savkin AN, Denisevich DS, Badikov KA, Sedov AA (2019) A new semi-analytical approach for obtaining crack-tip stress distributions under variable-amplitude loading. *Procedia Structural Integrity*, pp 684–687. <https://doi.org/10.1016/j.prostr.2019.05.085>
10. Savkin AN, Sunder R, Badikov KA, Sedov AA (2018) Fatigue crack growth kinetic on steels under variable amplitude loading. *PNRPU Mech Bull* 3:61–70. <https://doi.org/10.15593/perm.mech/2018.3.07>
11. Skorupa M (1998) Load interaction effects during fatigue crack growth under variable amplitude loading, a literature review. Part I .empirical trends. *Fatigue Fract Eng Mater Struct* 987–1006

12. Savkin AN, Sunder R, Denisevich DS, Sedov AA, Badikov KA (2018) Load interaction effects during near-threshold fatigue crack growth under variable amplitude: theory, model, experiment. *PNRPU Mech Bull* 4:246–255. <https://doi.org/10.15593/perm.mech/2018.4.22>
13. Bekal S (2013) Calculation growth on variable amplitude loading: master thesis. Manipal Institute of Technology, India, pp 112
14. Irwin GR (1957) Analysis of stresses and strain near the end of a crack traversing a plate. *J Appl Mech-Trans ASME* 24:351–369
15. Antunes FV, Souda T, Branco R, Corrieis L (2015) Effect of crack closure on non-linear crack tip parameters. *Int J Fatigue* 71:53–63
16. Arijit R, Manna I, Tarafder S, Sivaprasad S, Paswan S, Chattoraj I (2013) Hydrogen enhanced fatigue crack growth in an HSLA steel. *Mater Sci Eng* 588:86–96
17. Yang Y, Zhang W, Yongming L (2014) Existence and insufficiency of the crack closure for fatigue crack growth analysis. *Int J Fatigue* 62:144–153
18. Savkin AN, Sunder R, Andronik AV, Sedov AA (2018) Effect of overload on the near-threshold fatigue crack growth rate in a 2024–T3 aluminum alloy: I. effect of the character, the magnitude, and the sequence of overload on the fatigue crack growth rate. *Russ Metallurgy (Metally)* 11:1094–1099. <https://doi.org/10.1134/S0036029518110113>
19. Willenborg J, Engle RH, Wood HA (1971) A crack growth retardation model based on effective stress concepts. report AFFEL-TM-71-1- FBR, Dayton (OH): air force flight dynamics laboratory, wright-patterson air force base 9:15
20. Manjunatha CM (2008) Fatigue crack growth prediction under spectrum load sequence in an aluminum alloy by K^* -RMS approach. *Int J Damage Mech* 17:477–492
21. Carpinteri A, Spagnoli A, Terzano M (2019) Crack morphology models for fracture toughness and fatigue strength analysis. *Fatigue Fract Eng Mater Struct* 42(9):1965–1979. <https://doi.org/10.1111/ffe.13064>